Journal of Sound and Vibration (1997) **204**(2), 291–310

AXISYMMETRIC WAVE TRANSFER FUNCTIONS OF FLEXIBLE TUBES

R. J. PINNINGTON

Institute of Sound and Vibration Research, University of Southampton, Southampton, SO17 1BJ, England

(*Received* 9 *August* 1996, *and in final form* 29 *January* 1997)

The input and transfer impedances of fluid-filled pipes are calculated by using a wave approach. The pipe walls can have orthotropic elastic properties associated with braided rubber hose. The input and transfer impedances of a water-filled plain rubber hose are plotted for zero pressurization and positive and negative pressure. It is found that the pressure for this case does not greatly affect the stiffness. Input and transfer impedances are also plotted for a braided rubber hose which demonstrates the significant pressure stiffening effects found in practice.

1. INTRODUCTION

Elastomeric flexible tubes and bellows are used to control structure- and fluid-borne vibrational waves in pipes, and also to resolve alignment difficulties in construction. These elastomeric elements potentially provide an impedance mismatch, reflecting both fluid and structural waves back towards the source. In practice, however, the application has not been as successful as expected, because the stiffness or impedance of the element becomes large with increasing static pressure and also increasing frequency.

It is thought that these unwanted stiffening effects may be related to the steel or fibre braid within the elastomeric material. The braid is included to provide stiffening and strength while still permitting axial and lateral motion. The increase of stiffness with pressure may be on account of the tension within the braid causing waves to be controlled by membrane forces rather than bending forces. The stiffening effect observed with increasing frequency could well be a combination of the elastomer properties and increased radial restraint due to wall inertia.

This theoretical study is intended to investigate these phenomena by considering the general case of wave propagation in a fluid-filled, orthotropically stiffened and internally pressurized shell. Only axisymmetric waves were considered, as these are probably most significant, and a structure compliant enough to control these motions would imply adequate compliance of other wave types: in particular, the flexural wave.

In reference [1], the appropriate wave equations were set up. This led to plots of dispersion curves relating the wavenumbers of the four possible wave types to frequency. In general, two propagating waves occurred; one, denoted $s = 1$, was mainly in the fluid but involved significant radial wall motion, while the other, denoted $s = 2$, was mainly axial motion of the shell with little radial movement. The other two wave types $s = 3$ and $s = 4$ referred to bending waves which, below the ring frequency, were non-propagating waves seen as a local disturbance around axial discontinuities such as the input boundary.

0022–460X/97/270291 + 20 $25.00/0/sv970939

These dispersion relationships are used here to derive the impedance matrix for a fluid-filled tube. This matrix relates input fluid or structural motions to transmitted fluid pressures or axial wall stresses. The matrix could be coupled to a representation of other pipework to predict the overall attenuation of fluid- or structure-borne waves.

The impedance matrices of an elastomeric tube were calculated for zero internal pressure, and then positive and negative pressure. The pressurization caused some stiffening and softening changes.

A model [1], developed for the elastic moduli and Poisson ratio for wire-stiffened elastomer, exhibited the high coupling expected between the axial and radial motions of the tube wall. Impedance matrices for a pressurized braided tube were calculated which demonstrated more dramatic stiffness increases with pressure than had been seen with the unbraided tube in the earlier tests.

2. CALCULATION OF THE IMPEDANCE MATRIX FOR AN ELASTIC, FLUID-FILLED PIPE

Consider a fluid-filled pipe of finite length, l, which can be excited by axisymmetric forces or pressures at either end as shown in Figure 1. These forces could be an axial force, N, on the shell, a radial shear force, Q, a moment about a circumference, M, or a pressure force, P, acting on the fluid. The shell can respond in the axial or radial directions with displacements u and w. The fluid can move with an axial displacement u_f.

For the examples chosen here it is assumed that the flexible tube is clamped at either end to a stiffer pipe flange, thereby constraining the radial motion w and radial slope, $\partial\omega/\partial x$, to zero at these sections. No information will then be required concerning the associated radial shear force Q and moment M on the boundaries. The problem then reduces to the determination of the dynamic stiffness matrix in the equation

$$\begin{bmatrix} N_1 \\ P_1 \\ N_1 \\ P_2 \end{bmatrix} = \begin{bmatrix} K_{11} & \vdots & K_{12} \\ \cdots & \vdots & \cdots \\ K_{21} & \vdots & K_{22} \end{bmatrix} \begin{bmatrix} U_1 \\ U_{f1} \\ U_2 \\ U_{f2} \end{bmatrix}, \tag{1}$$

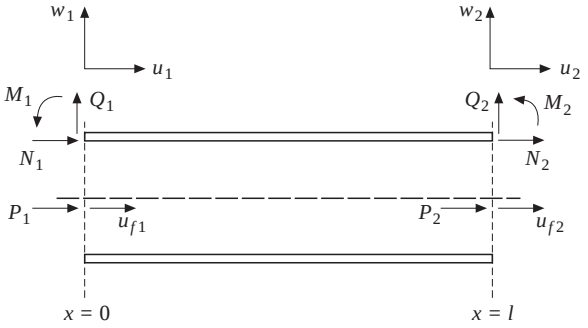

Figure 1. A section through a fluid-filled pipe, showing the sign convention.

TABLE 1

Physical parameters

	Rubber tube	Braided rubber tube
Pipe radius	25 mm	100 mm
Wall thickness	10 mm	10 mm
Pipe length	0·2 m	1 m
Plate modulus	$E'_x\,E'_\theta = 10^6$ N/m^2	$5{\cdot}1 \times 10^8$ N/m^2
Poisson ratio	$v_x, v_\theta = 0{\cdot}5$	$v_x, v_\theta = 1$
Wall density	10^3 kg/m^3	$1{\cdot}07 \times 10^3$ kg/m^3
Wall loss factor	0·1	0·1
Fluid loss factor	0·001	0·001
Fluid bulk modulus	$2{\cdot}7 \times 10^9$ N/m^2	$2{\cdot}7 \times 10^9$ N/m^2
Fluid density	10^3 kg/m^3	10^3 kg/m^3

in which the stresses and displacement are first given as a sum of wavenumber components, and then in terms of a common variable $\{w\}$, the radial displacement. Insertion of the boundary conditions at $x = 0$, $x = l$, gives the desired dynamic stiffness matrix and the impedance matrix (by a division by $i\omega$).

2.1. LIST OF SYMBOLS

The shell and fluid properties may be described by a set of non-dimensional parameters employed in reference [1]. These described the orthotropic properties of the shell, the internal pressure and axial tensile force, which are as follows.

Pipe dimensions: a = mean radius, h = wall thickness, l = length.

Material properties: ρ = shell density, ρ_f = fluid density, E'_x = elastic modulus of the shell in the x-direction, E'_θ = elastic modulus of the shell in the circumferential direction, v_θ, v_x = Poisson ratios, K_f = bulk modulus of the fluid, P_0 = static internal pressure, N_0 = tensile end force on the pipe.

Variables: f = frequency (Hz), $\omega = 2\pi f$ (frequency in rad/s), k_s = wavenumber of the sth wave, $\alpha_s = k_s a$ (non-dimensional wavenumber), $\Omega = \omega a\sqrt{\rho/E'_\theta}$ (non-dimensional frequency).

Non-dimensional parameters: $\gamma_p = P_0 a/E'_\theta h$ (normalized static pressure), $\gamma_E = E'_x/E'_\theta$ (elastic modulus ratio), $\psi = \Omega^2/\gamma_E\alpha_f^2 = (\rho/\rho f)/(B/(\gamma_E E_\theta))$ (the fluid wave speed normalized to the shell axial wave speed; $B = E'_x h^3/12$), $\chi = N_0/2\pi a E'_\theta h$ (the normalized tension/unit circumference), $c_1 = (v_x - \gamma_p)(v_\theta - \gamma_p/\gamma_E)$ (the lateral softening term due to pressure or Poisson ratio), $\beta = 2K_f a/E'_\theta h$ (the fluid loading term), $r = \gamma_E h^2/12a^2$ (normalized bending stiffness).

TABLE 2

Test parameters

Test	Pressure (bar)	γ_p	Tension (N)	χ	Figures
1	0	0	0	0	2–5
2	2	0·5	392	0·25	6
3	4	1	784	0·5	7, 8
4	−2	−0·5	−392	−0·25	9–11
5	0	0	0	0	12, 13
6	$5{\cdot}1 \times 10^6$	0·1	$1{\cdot}375 \times 10^5$	0·05	14, 16
7	$25{\cdot}5 \times 10^6$	0·5	8×10^5	0·25	17, 18

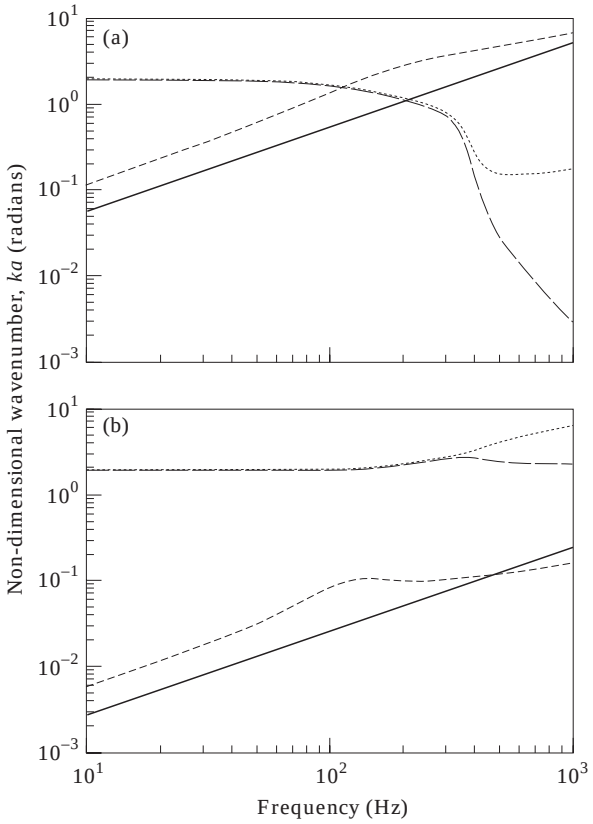

Figure 2. The non-dimensional wavenumber versus the frequency. Test 1, $\gamma_\rho = 0$, $\chi = 0$. ---, $s = 1$; ——, $s = 2$; — —, $s = 3$; · · · · ·, $s = 4$. (a) Real part; (b) imaginary part.

2.2. DERIVATION OF THE DYNAMIC STIFFNESS MATRIX

The axial displacement fields u and u_f, and the shell radial displacement W, may both be described as a sum of the four pairs of waves corresponding to the roots, $s = 1, 2, 3, 4$. The axial motion for the shell, for example, is

$$u = \sum_{s=1,4} [L_s] \begin{Bmatrix} U_s^+ \\ U_s^- \end{Bmatrix}, \tag{2}$$

where

$$[L_s] = \begin{bmatrix} e^{-ik_s x} & 0 \\ 0 & e^{ik_s x} \end{bmatrix}$$

and U_s^+ and U_s^- are the amplitudes of the right- and left-travelling waves. The radial shell displacement and fluid axial displacement are similarly written in terms of W_s^+, W_s^- and U_{fs}^+, U_{fs}^-.

If a travelling wave solution, $e^{-ik_s x}$, for a right-going wave is applied to the equation of axial equilibrium in the shell [1], equation (12) is then

$$\begin{Bmatrix} U_s^+ \\ U_s^- \end{Bmatrix} = \begin{bmatrix} C_s & 0 \\ 0 & -C_s \end{bmatrix} \begin{Bmatrix} W_s^+ \\ W_s^- \end{Bmatrix}, \tag{3}$$

where $C_s = \mathrm{i}\alpha_s(v_0 - \gamma_p/\gamma_E)/(\Omega^2/\gamma_E - \alpha_s^2)$.

The dynamic pressure, p, in the fluid can be described as the sum of the pressures,

$$p = \sum_{s=1,4} [L_s] \begin{Bmatrix} P_s^+ \\ P_s^- \end{Bmatrix}. \tag{4}$$

The pressures are related to the fluid axial velocities by

$$\rho_f \ddot{u}_f = -\partial p/\partial x. \tag{5}$$

For each wavenumber, s, the derivative is given as

$$\frac{\partial}{\partial x} \begin{Bmatrix} P_s^+ \\ P_s^- \end{Bmatrix} = -\frac{\mathrm{i}\alpha_s}{a} \begin{bmatrix} 1 & 0 \\ 0 & -1 \end{bmatrix} \begin{Bmatrix} P_s^+ \\ P_s^- \end{Bmatrix}. \tag{6}$$

For harmonic excitation, $\ddot{u}_{fs} = -\omega^2 U_{fs}\, \mathrm{e}^{\mathrm{i}\omega t}$, and equation (5) becomes

$$\begin{Bmatrix} P_s^+ \\ P_s^- \end{Bmatrix} = \begin{bmatrix} F_s & 0 \\ 0 & -F_s \end{bmatrix} \begin{Bmatrix} U_{fs}^+ \\ U_{fs}^- \end{Bmatrix}, \tag{7}$$

where $F_s = \mathrm{i}\omega^2 a\rho f/\alpha_s^2$ and P_s^- is the negative-going pressure wave.

In reference [1] the relationship between the pressure for the sth wave and the wall motion is given from radial equilibrium for both positive- and negative-going waves as

$$P_s = \frac{-2K_f}{1 - (\alpha_s/\alpha_f)^2} \frac{W_s}{a}. \tag{8}$$

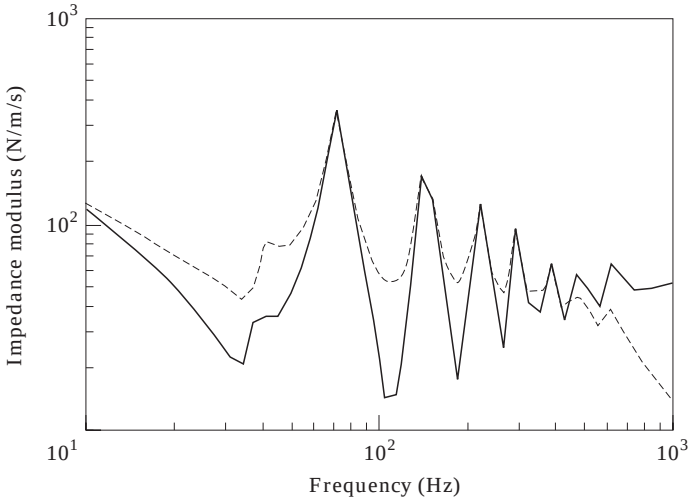

Figure 3. Test 1, $\gamma_\rho = 0$, $\chi = 0$; structural impedance modulus. ——. Input impedance, Z_{11}; - - - -, transfer impedance, Z_{12}.

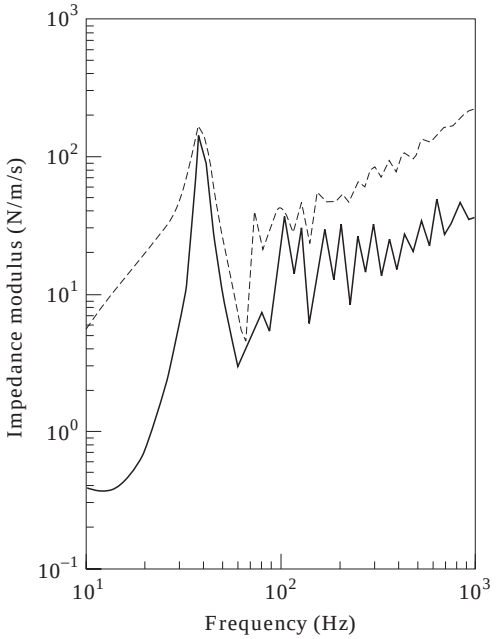

Figure 4. Test 1, $\gamma_\rho = 0$, $\chi = 0$; fluid input impedance, Z_{33}. ——, Real part; - - - -, modulus (water pipe = 2×10^3).

Therefore substitution of equation (7) into equation (8) gives

$$\begin{Bmatrix} U_{fs}^+ \\ U_{fs}^- \end{Bmatrix} = \begin{bmatrix} D_s & 0 \\ 0 & -D_s \end{bmatrix} \begin{Bmatrix} W_s^+ \\ W_s^- \end{Bmatrix}, \tag{9}$$

where $D_s = 2i\alpha_s/(\alpha_f^2 - \alpha_s^2)$.

The right- and left-going pressures can now be written by using equations (7) and (9) as

$$\begin{Bmatrix} P_s^+ \\ P_s^- \end{Bmatrix} = F_s D_s \begin{Bmatrix} W_s^+ \\ W_s^- \end{Bmatrix}. \tag{10}$$

The axial stress in the shell, σ_x, may also be described in terms of positive and negative travelling waves, σ_{xs}^+ and σ_{xs}^-, in the form of equation (2) within the framework of the Hooke's law relationship [1]:

$$\sigma_x = E_x'[\partial u/\partial x + v_\theta w/a]. \tag{11}$$

Upon using the differential operation of equation (6) on u, and making substitutions from equation (3), equation (11) becomes, in terms of the radial displacements,

$$\begin{Bmatrix} \sigma_{xs}^+ \\ \sigma_{xs}^- \end{Bmatrix} = \frac{E_x'}{a} (-i\alpha_s C_s + v_\theta) \begin{Bmatrix} W_s^+ \\ W_s^- \end{Bmatrix}. \tag{12}$$

The total axial stress, σ_x, at any point, x, can be expressed as the sum of four wave types

by using equation (12) by introducing the x-dependence vector in $[L_s]$ in equation (2):

$$\sigma_x(x) = \sum_{s=1}^{4} \frac{-E'_x}{a} (\alpha_s C_s - v_\theta)[1 \quad 1][L_s]\begin{Bmatrix} W_s^+ \\ W_s^- \end{Bmatrix}. \tag{13}$$

Likewise, the pressure at any point is

$$p(x) = \sum_{s=1}^{4} F_s D_s[1 \quad 1][L_s]\begin{Bmatrix} W_s^+ \\ W_s^- \end{Bmatrix}. \tag{14}$$

The axial displacement $u(x)$ in the shell is

$$u(x) = \sum_{s=1}^{4} C_s[1 \quad -1][L_s]\begin{Bmatrix} W_s^+ \\ W_s^- \end{Bmatrix}. \tag{15}$$

and the axial displacement in the fluid is

$$u_f(x) = \sum_{s=1}^{4} D_s[1 \quad -1][L_s]\begin{Bmatrix} W_s^+ \\ W_s^- \end{Bmatrix}. \tag{16}$$

The dynamic stiffness expressions require that the stresses and pressures are multiplied by the respective cross-sectional areas, such that the axial shell force, $N(x) = -2\pi ah\sigma(x)$, and the pressure force, $P(x) = \pi a^2 p(x)$. The matrices describing these forces at any position, x, are given from equations (13) and (14), so that

$$\begin{Bmatrix} N(x) \\ P(x) \end{Bmatrix} = [M][L]\{W\}, \tag{17}$$

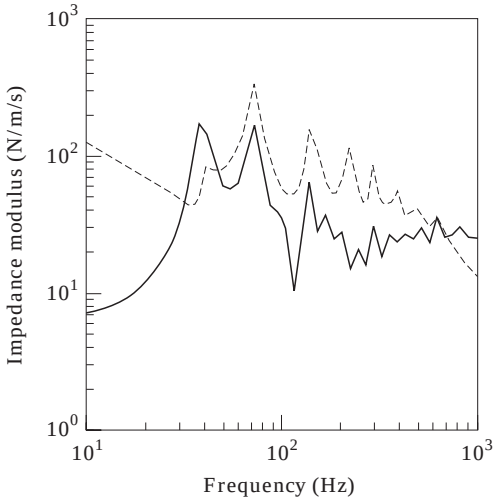

Figure 5. Test 1, $\gamma_\rho = 0$, $\chi = 0$; transfer impedance moduli. ——, Fluid, Z_{34}; - - - -, structural, Z_{12}.

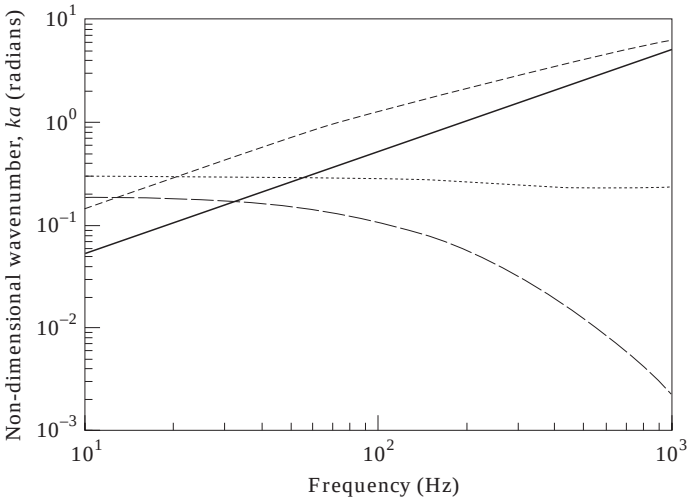

Figure 6. The non-dimensional wavenumber versus the frequency; real part. Test 2, $\gamma_\rho = 0{\cdot}5$, $\chi = 0{\cdot}25$. ---, $s = 1$; ——, $s = 2$; — —, $s = 3$; · · · · ·, $s = 4$.

where

$$[M] = [M_1 \quad M_2 \quad M_3 \quad M_4], \qquad M_s = \begin{bmatrix} 2\pi h E_x'(\alpha_s C_s - v_\theta) & 2\pi h E_x'(\alpha_s C_s - v_\theta) \\ \pi a^2 F_s D_s & \pi a^2 F_s D_s \end{bmatrix},$$

$$\underset{2 \times 8}{[L]} = \begin{bmatrix} L_1 & & & \\ & L_2 & & \\ & & L_3 & \\ & & & L_4 \end{bmatrix}, \qquad \underset{8 \times 1}{\{W\}} = \begin{Bmatrix} W_s^+ \\ W_s^- \\ \vdots \end{Bmatrix}, \qquad s = 1, 4.$$

The axial shell displacement and the fluid displacement at any section, x, can be similarly expressed by using equations (15) and (16):

$$\begin{Bmatrix} u(x) \\ u_f(x) \end{Bmatrix} = [N][L]\{W\}, \tag{18}$$

where

$$\underset{2 \times 8}{[N]} = [N_1 \quad N_2 \quad N_3 \quad N_4], \qquad [N_s] = \begin{bmatrix} C_s & -C_s \\ D_s & -D_s \end{bmatrix}.$$

Now that the displacements and the forces have been stated in terms of a common variable $\{W\}$, it is possible to write the dynamic stiffness matrix in the form shown in equation (1). This simply requires substituting into it the forces and displacements at the boundaries $x = 0,\ x = l$:

$$N_1 = N(0), \qquad N_2 = -N(l), \qquad P_1 = p(0), \qquad P_2 = -p(l),$$
$$U_1 = u(0), \qquad U_2 = u(l), \qquad U_{f1} = u_f(0), \qquad U_{f2} = u_f(l). \tag{19}$$

The forces at either end of the tube are given from equations (17) and (19):

$$\begin{Bmatrix} N_1 \\ P_1 \\ \cdots \\ N_2 \\ P_2 \end{Bmatrix} = \begin{bmatrix} [M] \\ \cdots\cdots\cdots \\ -[M][L(l)] \end{bmatrix} \{W\}. \tag{20}$$

The displacements at either end of the tube are likewise given from equations (18) and (19):

$$\begin{Bmatrix} U_1 \\ U_{f1} \\ U_2 \\ U_{f2} \end{Bmatrix} = \begin{bmatrix} [N] \\ \cdots\cdots\cdots \\ [N][L(l)] \end{bmatrix} \{W\}. \tag{21}$$

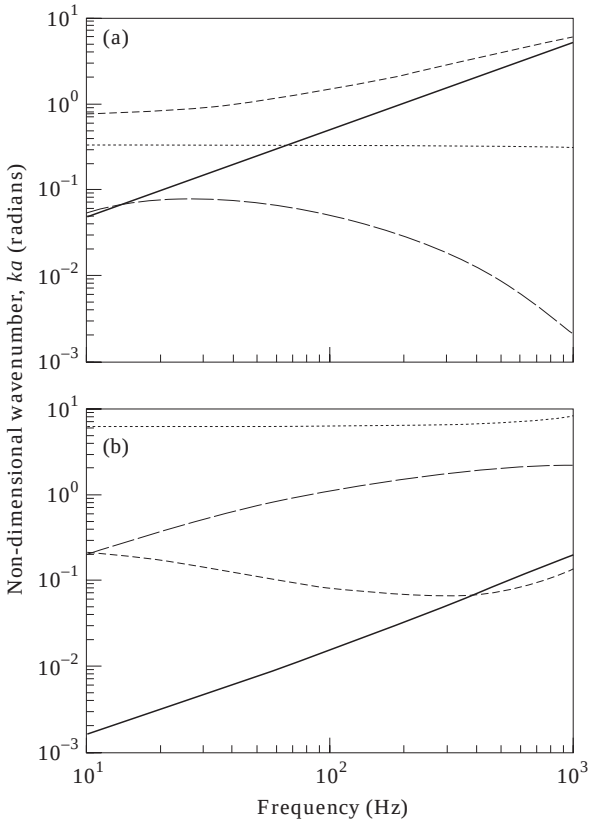

Figure 7. The non-dimensional wavenumber versus the frequency. Test 3, $\gamma_\rho = 1$, $\chi = 0{\cdot}5$. ---, $s = 1$; ——, $s = 2$; — —, $s = 3$; · · · ·, $s = 4$. (a) Real part; (b) imaginary part.

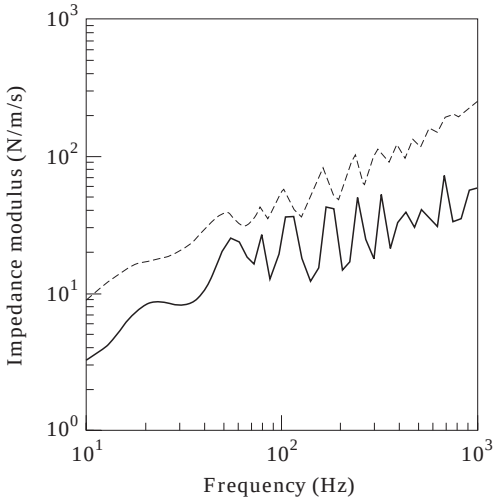

Figure 8. Test 3, $\gamma_\rho = 1$, $\chi = 0{\cdot}5$, fluid input impedance, Z_{33}. ---, Modulus; ——, real part.

The dynamic stiffness matrix is formed by eliminating $\{W\}$ from equations (20) and (21) by substitution into equation (1):

$$\begin{Bmatrix} N_1 \\ P_1 \\ N_2 \\ P_2 \end{Bmatrix} = \underset{4\times 4}{\begin{bmatrix} K_{11} & \vdots & K_{12} \\ & \vdots & \\ \cdots & \cdots & \cdots \\ & \vdots & \\ K_{21} & \vdots & K_{22} \end{bmatrix}} = \begin{Bmatrix} U_1 \\ U_{f1} \\ U_2 \\ U_{f2} \end{Bmatrix}, \tag{22}$$

where

$$\begin{bmatrix} K_{11} & \vdots & K_{12} \\ & \vdots & \\ \cdots & \cdots & \cdots \\ & \vdots & \\ K_{21} & \vdots & K_{22} \end{bmatrix} = \begin{bmatrix} [M] \\ \cdots \\ [M][L(l)] \end{bmatrix} \begin{bmatrix} [N] \\ \cdots \\ [N][L(l)] \end{bmatrix}^{-1}.$$

The impedance matrix $[Z] = (1/\mathrm{i}\omega)[K]$.

3. PROCEDURE

A series of computational parameter studies were conducted by using a program, written in MATLAB, on a water-filled rubber tube to identify the components of the impedance matrix. The transfer functions were produced for zero pressure, and also for positive and negative pressurization.

The effect of braided rubber was investigated by varying the shell orthotropic elastic moduli. Finally, the influence of pressure increase on the braided rubber shell was studied.

For each parameter set, the approach was to plot out the dispersion curves giving the wavenumber against frequency for the pipe under test. Dispersion curves against non-dimensional frequency were discussed in reference [1]. A matrix of wavenumbers against frequency was stored and applied to equation (22), thus calculating all the terms in the impedance matrix. Reciprocity checks were made between transfer functions confirming that $Z_{pq} = Z_{qp}$, where p and q are force and response co-ordinates.

3.1. TESTS ON A RUBBER TUBE

The physical parameters for the tests on a homogeneous rubber tube and a braided rubber tube are given in Table 1.

The pressure and axial tension were varied in the tests 1–6 as indicated in Table 2 for various pressures and tensions on a homogeneous rubber tube, with non-dimensional parameters γ_p and χ respectively given in section 2.1. The tension N_0 was obtained by closing the tube end and allowing the tube to resist the internal pressure, P. Therefore, in these tests tension was in a fixed relationship with the pressure, $N_0 = \pi a^2 P$, giving $\chi = 2\gamma_p$.

The significance of the normalized pressure is that values above unity are probably not obtainable because of catastrophic expansion for positive pressure. For negative pressure, $\gamma_p = -1$ will, very crudely, give buckling. Buckling is dependent on the wall thickness-to-radius ratio [3] and for decreasing wall thickness gives buckling $0 > \gamma_p > -1$.

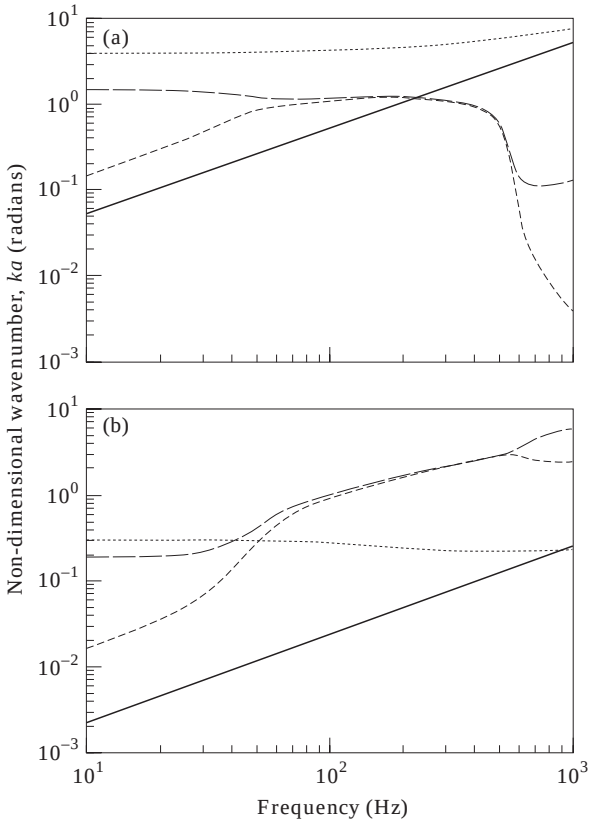

Figure 9. The non-dimensional wavenumber versus the frequency. Test 4, $\gamma_p = -0{\cdot}5$, $\chi = -0{\cdot}25$. ---, $s = 1$; ——, $s = 2$; — —, $s = 3$; · · · · ·, $s = 4$. (*a*) Real part; (b) imaginary part.

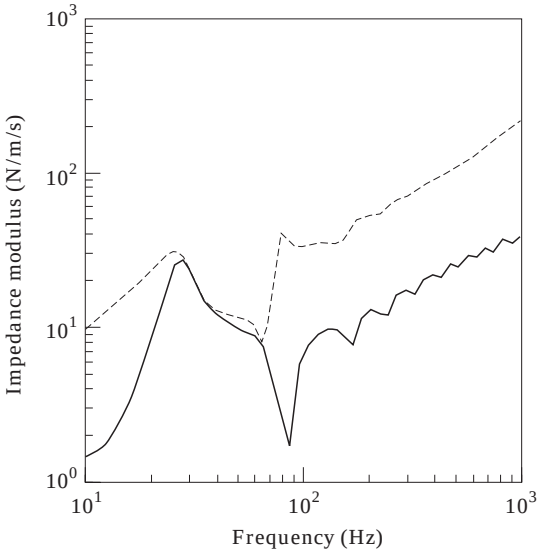

Figure 10. Test 4, $\gamma_\rho = -0{\cdot}5$, $\chi = -0{\cdot}25$, fluid input impedance, Z_{33}. ---, Modulus; ——, real part.

The preceding theory [1] also permitted calculations to be made on a wire stiffened or braided tube with anisotropic properties. The most interesting outcome of this analysis was that the Poisson ratio product, $v_\theta v_x$, of the composite tends towards unity as for a thickness constrained two-dimensional solid, as compared to a maximum of $v^2 = 0{\cdot}25$ for a homogeneous three-dimensional solid. In physical terms this means that axial and circumferential strains are strongly coupled in the stiffened material.

A parametric study described by tests 5–7 in Table 2 was conducted, in which the wavenumbers for various positive pressures and associated axial stresses were plotted from

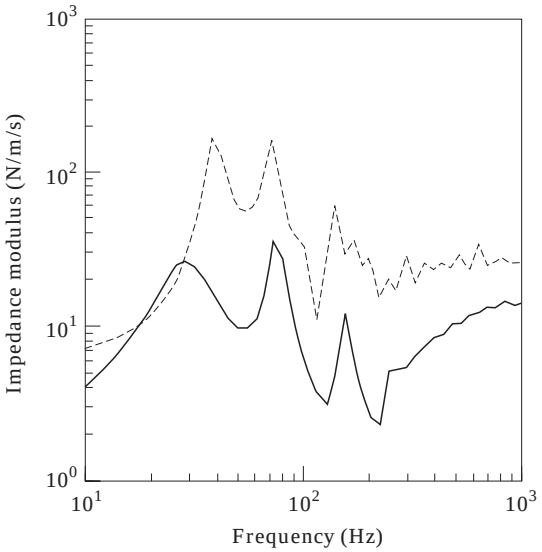

Figure 11. Test 4, $\gamma_\rho = -0{\cdot}5$, $\chi = -0{\cdot}25$. ——, Fluid transfer impedance Z_{34}; - - - -, structural Z_{12}.

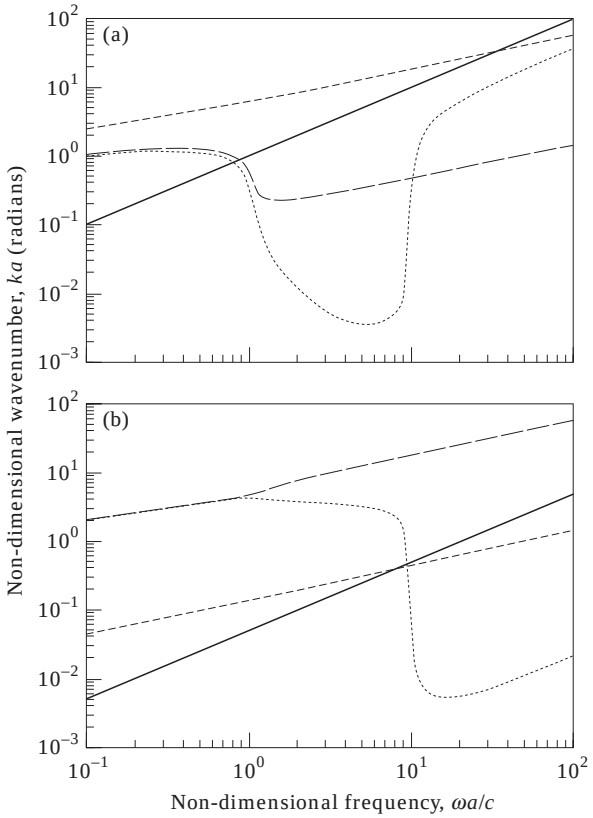

Figure 12. Test 7, $\gamma_\rho = 0$, $\chi = 0$; non-dimensional wavenumber. ---, $s = 1$; ——, $s = 2$; — —, $s = 3$; · · · · ·, $s = 4$. (a) Real part; (b) imaginary part.

which structural and fluid impedances were generated. The tube wall was rubber with 1% volume fraction steel wire inclined at 45° in both directions.

4. RESULTS AND DISCUSSION

4.1. POSITIVE AND NEGATIVE PRESSURIZATION OF A FLUID-FILLED RUBBER TUBE

4.1.1. *Zero pressure* ($\gamma_p = 0$), *zero tension* ($\chi = 0$): *test* 1

The real wavenumbers are seen in Figure 2(a). The $s = 2$ axial structural wavenumber in the shell increases linearly with frequency. The wave speed, c_2, is controlled by the Young's modulus of the rubber and the density of rubber $(E/\rho(1 - \nu^2))^{1/2}$. At 200 Hz the normalized wavenumber takes a value of unity indicating that this is the ring frequency for the tube.

The other propagating wave is that associated with the fluid mass and radial wall motion, denoted $s = 1$. The wavenumbers are about twice those of the structural wave, $s = 2$, up to the ring frequency. At frequencies below the ring frequencies, the $s = 1$ wave speed is controlled by the fluid mass and the wall radial modulus of elasticity, E'_θ. At higher frequencies the slope of this curve decreases as frequency to the power one half, indicating that the wall bending stiffness has become the controlling factor.

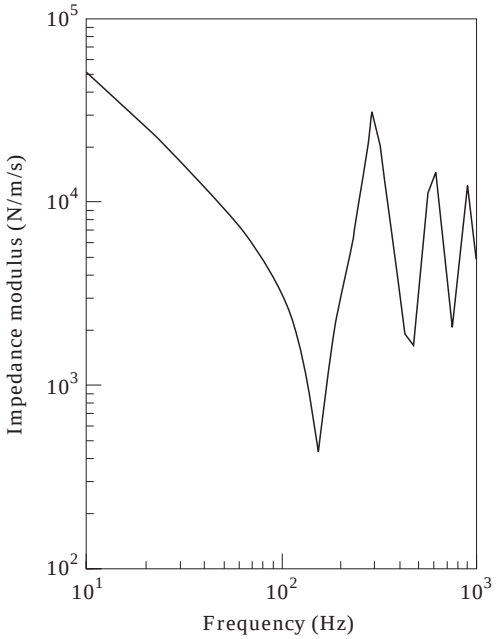

Figure 13. Test 7, $\gamma_\rho = 0$, $\chi = 0$, $\gamma_\rho = 0{\cdot}1$, $\chi = 0{\cdot}05$, $\gamma_\rho = 0{\cdot}5$, $\chi = 0{\cdot}25$. Structural input impedance, Z_{11}.

The other wavenumbers seen in Figure 2(a) are the real parts of complex waves which will be seen to be responsible for some local mass effects. The imaginary components of these waves are seen at the top of Figure 2(b). The attenuating parts of the propagating waves, $s = 1$, $s = 2$, due to material hysteresis, are in the lower section of Figure 2(b).

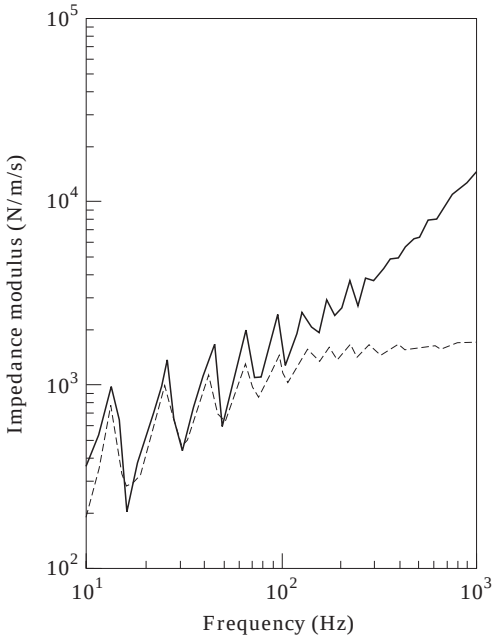

Figure 14. Test 7, $\gamma_\rho = 0$, $\chi = 0$. ——, Fluid input impedance, Z_{33}, - - - -, fluid transfer impedance, Z_{34}.

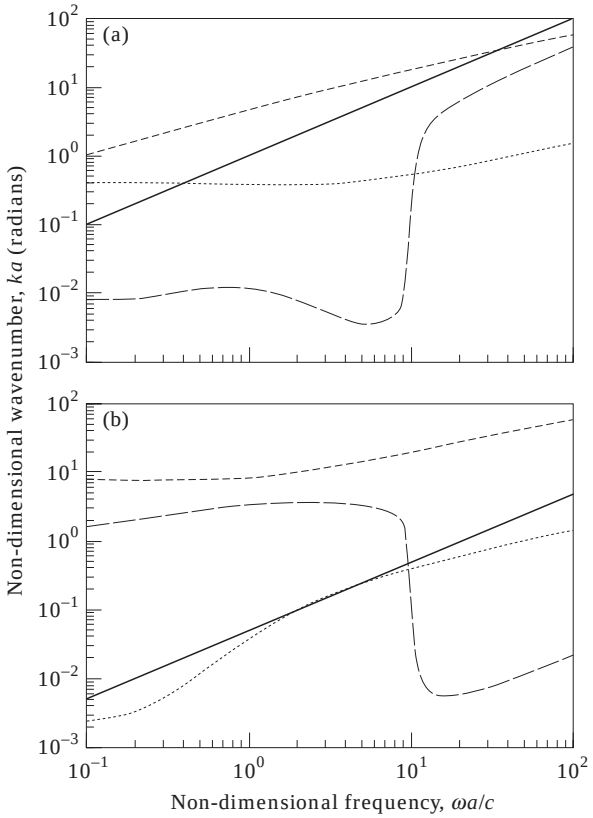

Figure 15. Test 8, $\gamma_\rho = 0{\cdot}1$, $\chi = 0{\cdot}05$; non-dimensional wavenumber against non-dimensional frequency. ---, $s = 1$; —, $s = 2$; — —, $s = 3$; · · · · ·, $s = 4$. (a) Real part; (b) imaginary part.

The impedance modulus, Z_{11}, for the axial structural input is displayed in Figure 3. The evenly spaced resonance peaks are associated with the structural wave, $s = 2$, discussed earlier. There is a stiffness characteristic at low frequencies giving a negative unit slope. The frequency average value, Z_s, is frequency independent with the form

$$Z_s = \rho c_2 A, \tag{23}$$

where A is the shell cross-sectional area and ρ is the wall density. The average value is about 40 N/ms. The frequency average value, Z_p, for a 6 mm wall steel pipe of the same 25 mm radius is 11×10^3 N/ms. This mismatch in characteristic impedances illustrates that the flexible tube would be a good reflection of structural waves like those in the steel pipe.

The structural transfer impedance, Z_{12}, describing the blocked force at the far end due to an input velocity at 1 is similar to the input impedance, Z_{11}, as would be the case for a longitudinal rod.

In Figure 4 is shown a display of the modulus of the input fluid impedance, Z_{33}, and the real part alone. The initial resonance at 30 Hz is also visible on the structural transfer function, Z_{11}, in Figure 3. The subsequent resonance peaks are closely spaced, as they are associated with the relatively high wavenumber of the fluid wave, $s = 1$. Below the ring frequency of 200 Hz the real component of impedance is constant, at about 10 N/ms. This is much less than the fluid impedance of a semi-infinite, hard-walled pipe of the same

radius, which has an input impedance of 2×10^3 N/ms. The flexible tube therefore has potential as an impedance mismatch device for fluid waves as well as structural waves.

At frequencies greater than 200 Hz the real part of the impedance increases slightly because the wall bending stiffness becomes dominant, as illustrated in the dispersion curve of the $s = 1$ wave.

Slightly detrimental to an impedance mismatch performance is the size of the imaginary component of the input impedance. This has a constant unit slope dominating the modulus curve. The ripples from the real part are still visible. The unit slope indicates that there is an attached mass effect of mass, m, with impedance, $i\omega m$. This is probably associated with the imaginary wave component with a value of 2 running across Figure 2(b).

In Figure 5 is shown the fluid transfer impedance, Z_{34}, taking, as expected, an almost constant value similar to that of the real part of the fluid input impedance, Z_{33}. The fluid and structural transfer functions are displayed together giving the relative sizes of transmitted forces when an equal velocity is imposed both on the fluid and structure at the free end. It is interesting that both contributions are of the same order of magnitude.

4.1.2. *Positive pressure* ($\gamma_p = 0{\cdot}5$), *positive tension* ($\chi = 0{\cdot}25$): *test* 2

This is a substantial pressure, close to the acceptable working limit of such a flexible tube as $\gamma_p = 1$ would probably correspond to bursting pressure. It is very interesting to see that there is again little discernible change to the dispersion curves in Figure 6, as compared to the unstressed version in Figure 2(a). The impedances, not shown here, are also very similar to those of the unstressed cases.

4.1.3. *Positive pressure* ($\gamma_p = 1$), *positive tension* ($\chi = 0{\cdot}5$): *test* 3

These static loads are probably not practical because it is thought that an instability could occur in the tube at this pressure causing an unlimited radial expansion.

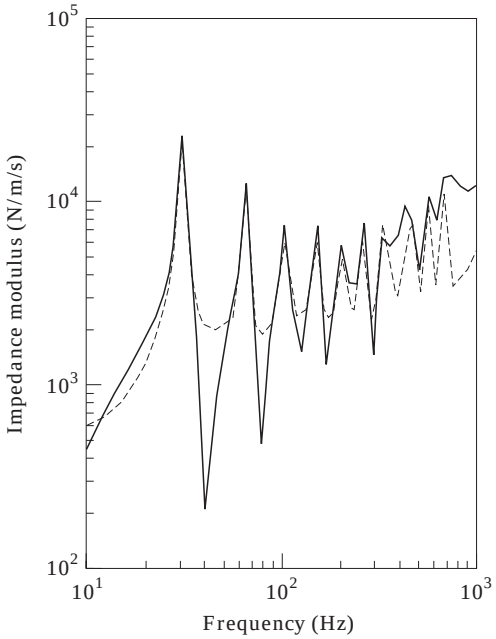

Figure 16. Test 8, $\gamma_p = 0{\cdot}1$, $\chi = 0{\cdot}05$. ——, Fluid input impedance, Z_{33}; ---, fluid transfer impedance, Z_{34}.

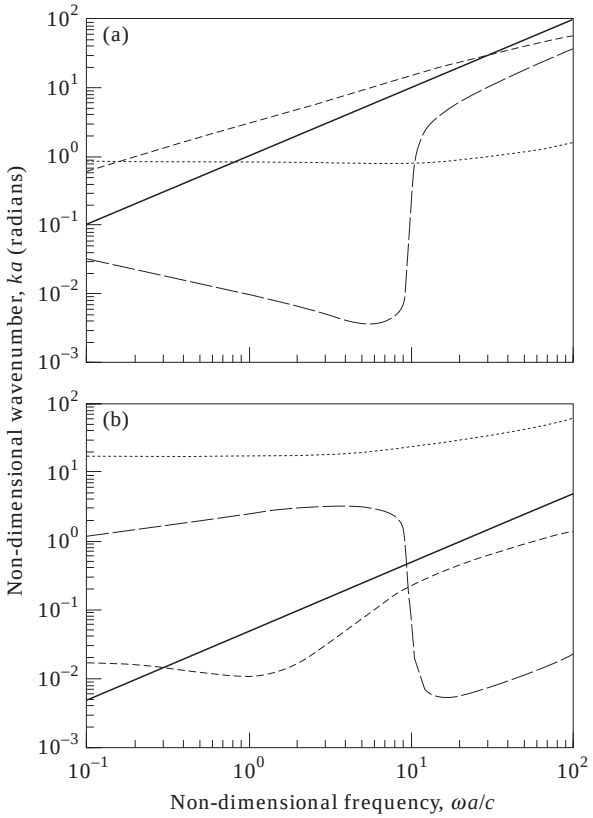

Figure 17. Test 9, $\gamma_p = 0{\cdot}5$, $\chi = 0{\cdot}25$; non-dimensional wavenumber against non-dimensional frequency. ---, $s = 1$; ——, $s = 2$; — —, $s = 3$; · · · · ·, $s = 4$. (a) Real part; (b) imaginary part.

The dispersion curves seen in Figure 7 have simplified. The $s = 2$ curve associated with the axial structural wave is unchanged. The $s = 1$ dispersion curve becomes horizontal at low frequencies with a value approaching unity.

The structural input impedance, Z_{11}, is unchanged from Figure 3, reflecting only axial wave motion. The fluid input impedance, Z_{33}, in Figure 8 is unchanged at high frequencies but softens considerably at low frequencies towards a minimum of 5 Hz, below which the behaviour is stiffness controlled. A zero at 0 Hz would imply instability because there is no stiffness. Therefore, in this case instability has not quite occurred, but is close.

4.1.4. *Negative pressurization* ($\gamma_p = -0{\cdot}5$) *and compressive axial force* ($\chi = -0{\cdot}25$): *test* 4

The dispersion curves for negative pressurization are given in Figures 9(a) and 9(b).

The $s = 2$ axial wave in the shell is not influenced by the negative pressure, the ring frequency is at 200 Hz as before, and the input structural impedance, Z_{11}, is unchanged from other cases.

Below the ring frequency the fluid wave $s = 1$ has slowed. There is also at the top of Figure 9(a) another curious wave type, $s = 4$, which has a bending wave characteristic at high frequencies. The significance of these modified waves is seen in the fluid input impedance, Z_{33}; see Figure 10. A couple of observations can be made using a comparison with the unpressurized example in Figure 4. The first resonance frequency has dropped slightly because of the increase in the fluid wavenumber, $s = 1$. The most noticeable effect,

however, is a dramatic increase in damping. The damping for the $s = 1$ wave becomes very large, seen by comparing the imaginary component with the real component. Equal magnitudes at about 100 Hz indicate a loss factor of unity. The fluid transfer impedance, Z_{34}, in Figure 11 is very interesting. There is a region of high attenuation between 30 Hz and 300 Hz compared with the unpressurized case. This is because the $s = 1$ fluid wave is not really propagating, but is rapidly attenuated by the high damping. The two resonances in this frequency range are associated with the axial structural wave, $s = 2$, visible in Figure 3. At frequencies above 300 Hz, the bending wave, $s = 4$, assumes significance and the transfer characteristic begins to rise.

These characteristics indicate that a negatively pressurized flexible tube could be a useful fluid pressure attenuation device if it could be correctly configured.

4.1.5. *Summary for the rubber pressurized flexible tube*

For positive pressurization, a rubber flexible tube appears to be a good impedance mismatch for both fluid and structural waves. Axial tension causes increased stiffness, but this is countered by the decreased stiffness from the internal pressure causing an increased radius. The upper pressure will be limited to the case when $\gamma_p = 1$ and instability will occur and the flexible tube in this linear model would expand uncontrollably.

Negative pressurization causes a softening in the fluid component of the impedance and a potential for high attenuation of fluid waves. The input impedance is, unfortunately, limited by an attached mass caused by flexural waves in the pipe wall. This limitation is not too serious, however, as the input impedance is always at least 0·1 of an equivalent fluid-filled, hard-walled tube.

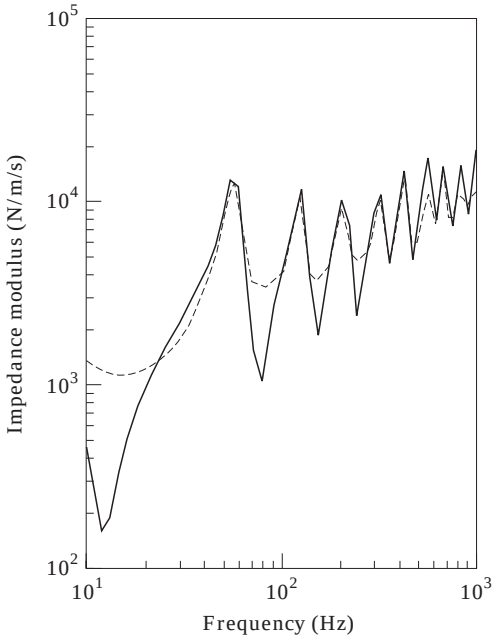

Figure 18. Test 9, $\gamma_p = 0{\cdot}5$, $\chi = 0{\cdot}25$. ——, Fluid input impedance, Z_{33}; ---, fluid transfer impedance, Z_{34}.

4.2. POSITIVE PRESSURIZATION OF A FLUID-FILLED, STEEL BRAIDED RUBBER TUBE

4.2.1. *Zero pressure* ($\gamma_p = 0$), *zero tension* ($\chi = 0$)

The dispersion curves for the braided rubber hose described in section 3 are shown in Figure 12. There are two propagating waves types, identified as those curves which have a real part much larger than the associated imaginary part.

The $s = 2$ axial structural wave is as before with the unstiffened rubber. It is a non-dispersive wave with a wavenumber of unit slope. The ring frequency occurs when the non-dimensional wavenumber is unity, as with all other cases.

The other propagating wave, denoted $s = 1$, is no longer a Korteweg type wave relying upon the wall elasticity, but rather a fluid-loaded, axisymmetric bending wave, of the sort seen before, only above the ring frequency. It is known to be bending in origin because of the slope of $(\text{frequency})^{1/2}$. This is the effect of braiding, which with water-filled tubes discourages radial expansion of the tube. Bending, the dominant motion, requires less stretching. The other two waves are complex and less significant.

The input structural impedance, Z_{11}, is displayed in Figure 13. It is, as expected, that of an equivalent rod in axial vibration. The frequency average impedance for this tube is 6×10^3 N/ms. The frequency average impedance for an equivalent steel tube of 6 mm wall thickness is 144×10^3 N/ms. This particular flexible tube would be quite effective at zero pressure as it offers a good impedance mismatch.

The input fluid impedance is shown in Figure 14. The increase of the average with frequency is consistent with behaviour dominated by axisymmetric bending waves. The impedance of an equivalent semi-infinite, fluid-filled, hard-walled tube is $4{\cdot}7 \times 10^4$ N/ms. Below about 300 Hz such a braided tube would give good attenuation because the impedance is at least one tenth that of the fluid. However, by 1000 Hz the flexible tube would not be very effective.

The fluid transfer characteristics in Figure 14 are fairly similar to the input characteristics discussed above, apart from the attenuation between input and output at high frequencies due to the damping.

4.2.2. *Positive pressure* ($\gamma_p = 0{\cdot}1$), *positive tension* ($\chi = 0{\cdot}05$)

The real wavenumbers for this case are in Figure 15 when the internal pressures and tensions are applied. The $s = 2$ axial structural wave and the associated input structural impedance seen in Figure 13 are unaffected, as with all previous examples.

The reason that the axial structural wave never changes is that the water within the tube prevents radial wall motion for this wave type. The wave is therefore not affected by out-of-plane bending forces or membrane forces. It should be noted that for test purposes, pipe flexibles are often pressurized with air rather than water which would permit radial wall motion and so appear to be softer. Such tests would give an exaggerated view of the flexible's isolating potential. When pressurization is applied, or as frequencies increase, the radial wall motions become restricted and the tube stiffens.

The $s = 1$ wavenumber, the upper curve in Figure 15, is one-third of the unpressurized low frequency value, indicating considerable stiffening. The slope changes to become proportional to frequency suggesting that pressure related membrane forces control the response rather than the bending waves of the unpressurized case.

These observations are borne out by the forms of the input and transfer fluid impedances given in Figure 16. The average values have risen at lower frequency by a factor of ten, causing a deterioration of the impedance mismatch performance.

These results are very interesting, because they suggest that the stiffening observed under pressurization could be indeed due to the braiding. The braiding has a high Poisson ratio,

of order unity, describing a strong interdependence between radial and axial motion. The restraint of radial expansion causes axial tensile forces which in turn stiffen the tube. Unbraided rubber does not exhibit this phenomenon to the same extent because the Poisson ratio is of the order of 0·5, describing a reduced radial to axial coupling.

4.2.3. *Positive pressure* $\gamma_p = 0{\cdot}5$, $\chi = 0{\cdot}25$

Further increase of the pressure causes no change to the structural input impedance, Z_{11} (see Figure 17), but results in further stiffening to the fluid waves as expected (see Figure 18). Comments are the same as for the previous example.

5. CONCLUSIONS

Some theory and computer modelling was completed to generate the impedance matrix of a pressurized elastic tube. It was found that for positive pressurization a rubber tube did not stiffen much with increasing frequency and, in principle, could be used as an effective impedance mismatch device for both fluid and structural vibration in pipes.

A model was developed for the elastic properties of a wire stiffened rubber tube. It was found that a Poisson ratio approaching unity could be obtained. This means that lateral and axial motion of the tube are highly coupled. For the wire stiffened tube it was found that the stiffness was increased significantly by internal pressure. This is because the tension in the wires now controls the tube dynamic behaviour. Stiffness is therefore proportional to tension or internal pressure.

If axial vibration tests are conducted on an air-filled tube, an unrepresentatively low stiffness will be recorded in comparison to that for a liquid within as the liquid restrains the radial motion.

The fluid and structural impedance matrix for a negatively pressurized rubber tube was generated. The tube softened under pressure, causing attenuation to travelling waves in the fluid. The input characteristics did not change greatly with pressure because there is an attached mass effect associated with non-propagating bending waves in the shell. In practice, negatively pressurized rubber tube was more likely to have bending instability problems.

REFERENCES

1. R. J. Pinnington 1997 *Journal of Sound and Vibration* **204,** 271–289. The axisymmetric wave transmission properties of pressurized flexible tubes.
2. P. B. Lindley 1964 *NR Technical Bulletin*, *Malaysian Rubber Producers Research Association*. Engineering design with natural rubber.
3. S. Timoshenko 1936 *Theory of Elastic Stability*. New York: McGraw-Hill.